Nigerian Research Journal of Chemical Sciences (ISSN: 2682-6054)
Volume 13, Issue 2, 2025

Synthesis, Characterization and *In Silico* Studies of Organosilane Schiff Bases Derived from 3-Aminopropyltrialkoxysilanes

Ugwu Ejiofor Everistus, Oruma Uchechukwu Susan, Ikechukwu Irene Uchechi,
Asegbeloyin Jonnie Niyi. and *Obasi Nnamdi Lawrence
Department of Pure and Industrial Chemistry,
University of Nigeria, Nsukka.
Corresponding Author: nnamdi.obasi@unn.edu.ng

Accepted: September 20, 2025. Published Online: September 26, 2025

ABSTRACT

Organosilane Schiff bases (four) namely; (E)-1-(2-nitrophenyl)-N-3-(triethoxysilyl)propyl) methanimine (BAPTE), (E)-1-3-nitrophenyl)-N-3-(triethoxysilyl) propyl methanimine (TAPTM), (E)-N,N-dimethyl-4-(((3-(triethoxysilyl)propyl)imino)methyl) aniline (PAPTE), and (E)-2-methoxy-5-(((3triethoxysily)propyl) imino) methyl) phenol (HAPTE) were synthesized by the condensation reaction of substituted benzaldehydes and derivatives of aminosilanes. The compounds were characterized by texture, solubility, melting point, FTIR, ^{1}H, and ^{13}C NMR spectroscopies. The spectral data gave evidence for the formation of azomethine group. The *in silico* studies were performed using the expanded force field version of autodockvina (autodockvina 1.2.0). The results revealed that the binding energies obtained for all synthesized compounds were lower than those of the reference compounds (Clociguanil and Cycloguanil). This implies that the synthesized compounds are more stable in the target than the reference compounds and may possibly elicit better therapeutic effects. Furthermore, the *in silico* results indicated that all the synthesized compounds were not inhibitors to the five most important Cytochrome P450 enzymes known to metabolize 90% of drugs. This implies that the compounds can be metabolized and excreted from the body if used as drugs.

Key words: Antimalarial activity, *in silico*, organosilanes, Schiff bases, spectroscopy.

INTRODUCTION

Schiff bases are derivatives of aldehydes or ketones, where the C=N-R group replaces the C=O group [1]. first preparation of imines was reported in the 19th century by Hugo Schiff [2]. Since then, a variety of methods for the synthesis of imines have been described [3]. Organosilanes, on the other hand, are compounds derived from silane. A defining characteristic of organosilanes is

that they must be organic and contain at least one carbon–silicon bond (C-Si). These compounds can effectively couple organic polymers with inorganic materials [4]. Organosilanes have a variety of applications, including serving as long-lasting hydrophobing agents in concrete construction and as coupling agents [5].

Malaria has posed a threat to humanity. The global emergence of antimicrobial resistance, particularly in malaria, underscores the need for intensive research to discover novel antimicrobial agents [6]. Schiff bases have demonstrated a promising range of biological properties. Moreover, organosilane-derived Schiff bases play an intriguing biological role in living organisms. However, a comprehensive understanding of their structure-activity relationships remains challenging and is yet to be fully established [7, 8].

In view of this, Schiff bases derived from 3-aminopropyltrialkoxysilanes were synthesized, characterized, and investigated for *in silico* activities.

MATERIALS AND METHODS

^{1}H-NMR and ^{13}C-NMR spectroscopies of the compounds were obtained on a Bruker 400 MHz and 300 MHz spectrometer respectively, $DMSO_6$ and CDC_3 were used as solvents for all ligands. The infrared spectra were recorded in the range of 4000-400 cm^{-1} using KBR pellets in Shimadzu spectrophotometer. Melting points were obtained with a Fisher John's melting point apparatus.

Synthesis of (E)-1-(2-nitrophenyl)-N-3-(triethoxysilyl)propyl)methanimine (BAPTE)

2-nitrobenzaldehyde (0.01 mol, 1.51 g) was dissolved in toluene (10 mL), and 3-aminopropyltriethoxysilane (0.01 mol, 2.34 mL) was dissolved in toluene. The resulting solutions were mixed; the mixture was further stirred under reflux in a water bath at 75 °C. It was left for some minutes, and a yellow precipitate was formed which was washed with methanol and in a desiccator (Scheme 1).

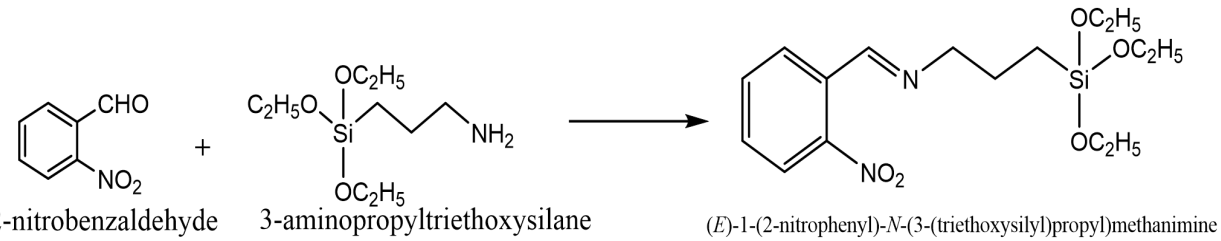

2-nitrobenzaldehyde 3-aminopropyltriethoxysilane (*E*)-1-(2-nitrophenyl)-*N*-(3-(triethoxysilyl)propyl)methanimine

Scheme 1: Synthesis (E)-1-(2-nitrophenyl)-N-(3-(triethoxysilyl)propyl)methanimine

Synthesis of (E)-1-(3-nitrophenyl)-N-3-(triethoxysilyl)propyl)methanimine (TAPTM)

3-nitrobenzaldehyde (0.01 mol, 1.51 g) was dissolved in toluene (10 mL) and 3-aminopropyltrimethoxysilane (0.01 mol, 1.74 mL) was dissolved in toluene. The resulting solutions were mixed; the mixture was further stirred under reflux in a water bath maintained at 75 °C for 2 h. It was left for some time, and a pale yellow solid was formed, which was filtered and stored in a desiccator (Scheme 2).

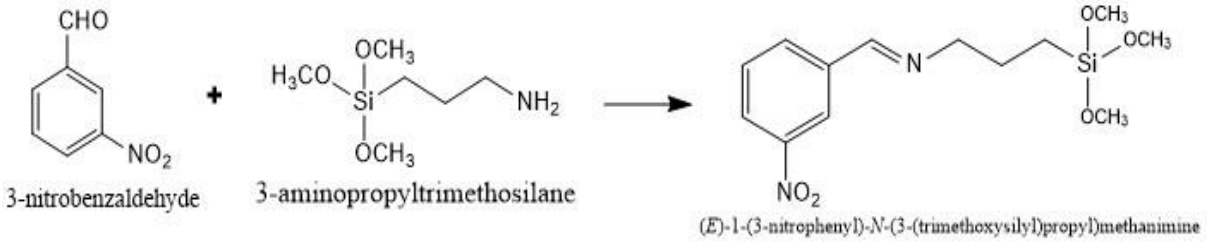

Scheme 2: Synthesis of (E)-1-(3-nitrophenyl)-N-3-(triethoxysilyl)propyl)methanimine

Synthesis of (E)-N-N-dimethyl-4-(((3-(triethoxysilyl)propyl)imino)methyl)aniline (PAPTE)

p-dimethylbenzaldehyde (0.01 mol, 1.49 g) was dissolved in methanol (10 mL) and 3-aminopropyltriethoxysilane (0.01 mol, 2.34 mL) was dissolved in toluene. The resulting solutions were mixed; the mixture was further stirred under reflux in a water bath maintained at 75 °C for 2 h. It was left overnight, and a yellow solid formed, which was washed with methanol and in a desiccator (Scheme 3).

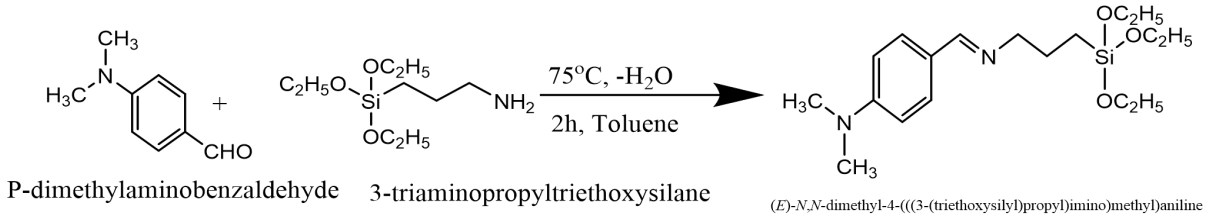

Scheme 3: Synthesis of (*E*)-N-N-dimethyl-4-(((3(triethoxysilyl)propyl)imino) methyl)aniline

Synthesis of (E)-2-methoxy-5-(((3-(triethoxysilyl)propyl)imino)methyl)phenol (HAPTE)

3-hydroxy-4-methoxybenzaldehyde (0.01 mol, 1.52 g) was dissolved in methanol (10 mL) and 3-aminopropyltriethoxysilane (0.01 mol, 2.34 mL) was dissolved in toluene. The resulting solutions were mixed; the mixture was further stirred under reflux in a water bath maintained at 75 °C for 2 h. It was left overnight, and a pale-yellow solid was formed, which was washed with methanol and in a desiccator (Scheme 4).

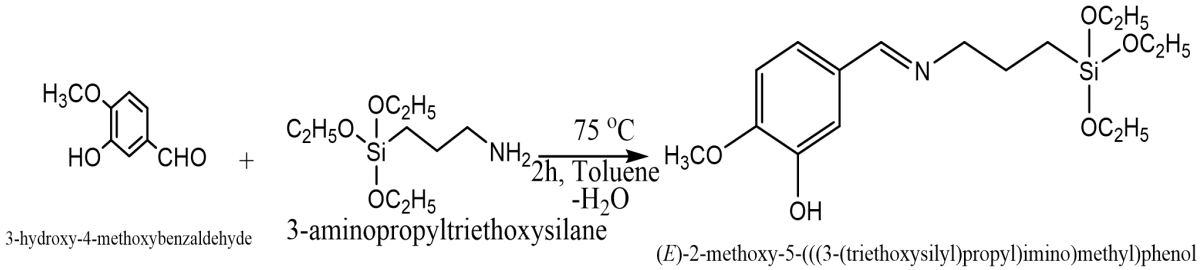

Scheme 4: Synthesis of (*E*)-2-methoxy-5-(((3-(triethoxysilyl)propyl)imino)methyl)phenol

Preparation of protein target

The wild-type *Plasmodium falciparum dihydrofolate reductase-thymidylate synthase* which is an experimentally validated target for antifolate antimalarials was chosen for this study [9]. It is a dimeric protein enzyme and as a result, the chain A was chosen for molecular docking. The protein was prepared using Autodock tools (1.5.6) [10]. Water molecules, lone pairs, non-standard residues and non-polar hydrogens were removed. Gasteiger charges and polar hydrogens were added. The active sites according to previous study [9] were selected and the grid box was set around the region which results in the chosen gridbox configuration and was preserved for virtual screening as shown in Table 1.

Table 1: Grid box dimensions for virtual screening study

Receptor	PDB ID	Grid box configurations (XYZ coordinates)				
		Grid points	X	Y	Z	Grid spacing (Å)
PfDHFR-TS	1J3I	60×60×60	28.947	28.905	9.667	0.375

Docking studies

Docking of the synthesized compounds was carried out using the expanded force field version of autodockvina (autodockvina 1.2.0). This newly released version has improved features including parameters for silicon atom [11]. It utilizes the Monte-Carlo iterated search algorithm.

Post docking visualization

The structures of the conformation of the docked synthesized compounds complexed with the receptor macromolecules were retrieved and the poses were visualized. The ligand-receptor complexes were further analyzed for the receptor-ligand interactions (with the binding site

residues), in Discovery Studio Visualiser 2020 [12]. Among multiple interactions, non-covalent interaction, including the occurrences of conventional hydrogen bond, Vanderwaal, π–π, π-sigma bond, π-sulfur, and many other hydrophobic interactions among the other existing ones were considered [13].

Drug likeliness, pharmacokinetics and Admet properties

The drug likeliness and pharmacokinetics of the six compounds were predicted using SwissADME[14]. CarcinoPred-EL [15], a web-based tool, was used to predict the carcinogenicity.

Toxicity prediction

The oral rat acute toxicity LD_{50} was determined using PkCSM, a toxicity prediction tool which employs graph-based signatures. It also predicted the Maximum tolerated dose in humans [15].

RESULTS AND DISCUSSION

FT-IR studies

The characteristic infrared data of the compounds reveal a band at 3021 cm^{-1} that was attributed to υ(Ar-CH). Strong bands ascribed to the azomethine υ(HC=N-) stretching of all the ligands at approximately 1632–1601 cm^{-1}. The Si-O bands in the ligands are what caused the medium bands at 1307–1024 cm^{-1}. The strong and broad band at 3540 cm^{-1} for the ligand HAPTE was due to υ(OH) stretching. The spectra at 2982-2800 cm^{-1} for the ligands were attributed to υ(aliph.CH) stretching. The bands that occurred in the range 1549-1314 cm^{-1} for BAPTE were attributed to the nitro group in the ligand. The summarized IR spectral results of the compounds are displayed in Table 2, while the spectra can be found in the supplementary information (Figures S1-S4).

Table 2: IR spectral data of the compounds (cm^{-1})

Compounds	υ(OH)	υAr(C-H)	υaliph.(C-H)	υHC=N)	υ (Si-O)	υ(NO_2)
HAPTE	3540br	3278m	2849-2800m	1621s	1307m	
BAPTE	-	3095m	2982-2827m	1623s	1024m	1489-1352m
TAPTM	-	3048w	2916-2820m	1617s	1065m	1549-1314m
PAPTE	-	3082w	2909-2822m	1604s	1065m	-

Key: s = strong, m = Medium, w = weak, br = broad

NMR studies

The multiple signals observed in the ^{1}H NMR spectrum in the range 6.50-8.45 ppm were attributed to the aromatic protons (Ar-H) for all the compounds synthesized. The compounds BAPTE and PAPTE exhibit triplet signals within 1.20-1.85 ppm and quartet signals within 3.20-3.45 ppm attributed to ($-OCH_2CH_3$) protons. The ($Si-(CH_2)_3$) protons signals were observed within 0.32-3.52 ppm for all the compounds. The triplet signal observed at 3.65 ppm correspond to the ($-OCH_3$) protons of TAPTM. The singlet signal at 10.00 ppm for HAPTE is attributed to the –OH group. The singlet signals observed between 7.75 – 8.80 ppm correspond to the azomethine proton (CH=N) for all the compounds synthesized.

In the ^{13}C NMR analysis, BAPTE exhibits a signal at 154.67 ppm, which is assigned to the azomethine carbon atom (HC=N). Phenyl carbon atoms were identified as the source of the signal at 111.53–132.00 ppm, while aliphatic carbon atoms were responsible for the signals at 39.49 – 40.49 ppm.The carbon atom of the methoxy group ($-OCH_3$) led to the signal at 55.68 ppm. The signals from 114.53–153.68 ppm originated from the phenyl carbon atoms, while the signals between 39.49 and 40.47 ppm were attributed to aliphatic carbon atoms. The azomethine carbon atom (HC=N) is responsible for the BAPTE signal at 154.67 ppm. Phenyl carbon atoms were identified as the source of the signal at 111.53–132.00 ppm, while aliphatic carbon atoms were responsible for the signals at 39.49 – 40.49 ppm.

The HAPTE compound showed a signal at 160.48 ppm represented the azomethine carbon atom (HC=N), the signals at 39.49 – 40.49 ppm represents aliphatic carbon atoms, and the signals at 111.63–153.82 ppm represents aromatic carbon atoms. The azomethine carbon atom (HC=N) was identified in the PAPTE as having a signal at 154.65 ppm. The aromatic carbon atoms were responsible for the signals at 111.53–132.0 ppm, and the aliphatic carbon atoms were identified by the signals at 39.49 – 40.49 ppm.

The TAPTM indicated that aliphatic carbon atoms were responsible for signals at 39.46–40.49 ppm, whereas aromatic carbon atoms were linked to signals at 111.27–132.02 ppm. All the ^{1}H and ^{13}C NMR spectra can be found in the supplementary information (Figures S5-S12).

Molecular Docking

All synthesized compounds were predicted to have high gastric intestinal absorption which is a property that suggests high bioavailability of the compounds. Not being permeability

glycoprotein (P-gp) [16] substrate implies that these compounds will not be subjected to efflux out of the target cells. P-gp is a protein that pumps foreign substances out of the cells. It recognizes some drugs as foreign substances and tend to pump them out of the target cells thereby reducing the therapeutic efficiency of the drug. Drugs that are not P-gp substrates would have better bioavailability.

The binding energies obtained for all synthesized compounds were lower than that of the reference compounds (Clociguanil and Cycloguanil) as shown in Table 4. This implies that the synthesized compounds were more stable in the target than the reference compounds and would possibly elicit a better therapeutic effect. As a result of post-docking visualization, ligand-protein bonds with the following interactions were found: alkyl, pi-alkyl, carbon hydrogen, van der Waals, conventional hydrogen bond, pi-pi stacked, amide-pi stacked, and pi-sulphur.

The presence of hydrogen bond in this interaction measures the stability of ligand-protein interaction since this was the strongest bonds among other interactions. CYP1A2, CYP2C19, CYP2C9, CYP2D6 and CYP3A4 are among the most important Cytochromes P450 that metabolize about 90 % of drugs [17]. All of the compounds were not inhibitors of at least one of these enzymes, as can be seen from the results displayed in Table 5, suggesting that if the compounds were used as drugs, they could be metabolized and eliminated from the body. Many interactions were seen after post-docking visualization (2D and 3D visualization) as shown in Table 6.

These interactions included van der Waals, conventional hydrogen bond, carbon-hydrogen, Pi-Pi stacked, amide-Pi stacked, alkyl, Pi-alkyl, and Pi-sulphur ligand-protein bonds as shown in Figures 1(a) and (b).

The presence of hydrogen bond in this interaction measures the stability of ligand-protein interaction since this was the strongest bonds among other interactions. In this interaction it was observed that, with the exception of compound PAPTE, all other compounds interacted with ALA16 amino acid while with the exception of compound TAPTM, all other compounds interacted with PHE58. Also, conventional hydrogen bond which was the strongest bond among other interactions was observed in compounds: HAPTE, BAPTE and TAPTM.

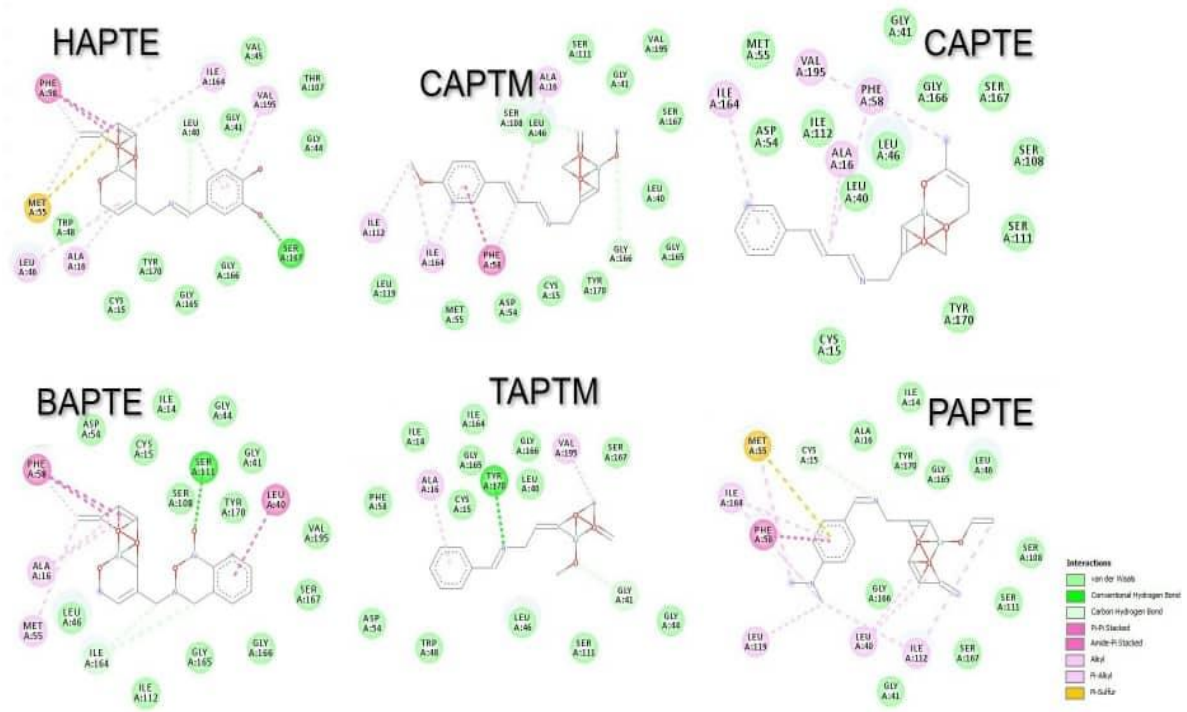

Figure 1 (a): 2D representation of the interactions between compounds and the receptor (PfDHFR-TS)

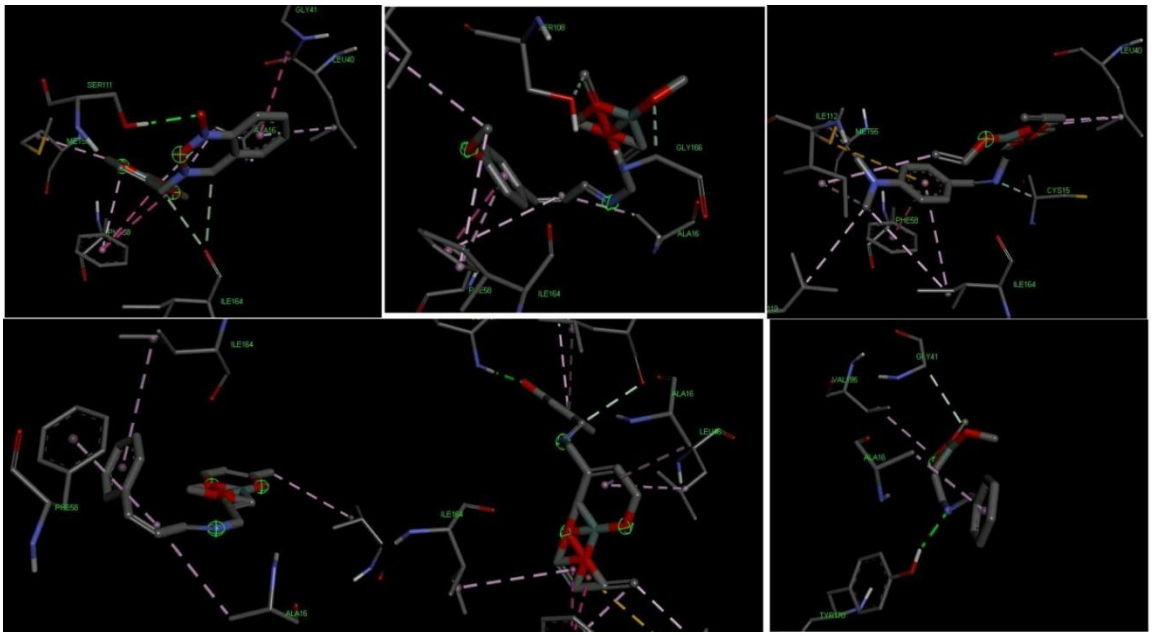

Figure 1 (b). 3D representation of the interactions between compounds and the receptor (PfDHFR-TS)

Table 3: Predicted toxicity of synthesized compounds

Compound	Ames toxicity	Oral rat acute toxicity LD50 (mol/kg)	Max. tolerated dose human (log mg/kg/day)	Carcinogenicity
HAPTE	No	2.099	0.699	N
BAPTE	No	2.518	0.744	N
TAPTM	No	2.535	0.848	N
PAPTE	No	2.207	0.809	C

Table 4: Predicted physicochemical properties of synthesized compounds

Compound	Binding energy	Molecular weight	Rotatable bonds	H-bond acceptor	H-bond donor	Logp
HAPTE	-8.623	341.47	11	6	2	2.23
BAPTE	-9.450	354.47	12	6	0	2.47
TAPTM	-6.853	267.4	8	4	0	2.01
PAPTE	-8.116	352.54	12	4	0	3.05
Clociguanil	-6.776	316.19	3	3	2	1.87
Cycloguanil	-6.746	251.72	1	2	2	1.35

Table 5: Predicted pharmacokinetics and drug likeliness of synthesized compounds

Solubility class	GI absorption	BBB permeant	P-gp substrate	CYP1A2 inhibitor	CYP2C19 inhibitor	CYP2C9 inhibitor	CYP2D6 inhibitor	CYP3A4 inhibitor
Slightly soluble	High	No	No	No	No	No	Yes	No
Slightly soluble	High	No	No	Yes	Yes	No	No	No
Soluble	High	Yes	No	No	Yes	No	No	No
Slightly soluble	High	Yes	No	No	No	No	Yes	Yes

Table 6: Binding interactions of the docked compounds with *Plasmodium falciparum dihydrofolate reductase-thymidylate synthase*

Compound	Bond	Amino acid residues
HAPTE	van der waals, conventional hydrogen bond, carbon hydrogen bond, pi-sulfur, pi-pi stacked, alkyl and pi-alkyl bond	ALA16, LEU40, LEU46, MET55, PHE58, ILE164, VAL195, SER167
BAPTE	van der waals, conventional hydrogen bond, carbon hydrogen bond, pi-pi stacked, amide-pi stacked, alkyl and pi-alkyl bond	ALA16, LEU40, GLY41, MET55, PHE 58, SER111, ILE164
TAPTM	van der waals, conventional hydrogen bond, carbon hydrogen bond, alkyl and pi-alkyl bond	ALA16, GLY41, TYR170, VAL195
PAPTE	van der waals, carbon hydrogen bond, pi-sulfur, pi-pi stacked, alkyl and pi-alkyl bond	CYS15, LEU40, MET55, PHE58, ILE112, LEU119, ILE164

CONCLUSION

Four organosilane compounds, E-1-(2-nitrophenyl)-N-3-(triethoxysilyl) propyl methanimine (BAPTE), E-1-(3-nitrophenyl)-N-3-(triethoxysilyl) propyl methanimine (TAPTM), E-N,N-dimethyl-4-(((3-(triethoxysilyl) propyl)imino) methyl) aniline (PAPTE), and E-2-methoxy-5-(((3-triethoxysilyl) propyl)imino) methyl) phenol (HAPTE) was prepared. FT-IR, ^{1}H, and ^{13}C NMR spectroscopies were employed to characterize these compounds. The Schiff bases derived from 3-aminopropyltrialkoxysilanes have shown significant potential for various applications due to their unique properties.

The synthesis of these compounds involves a straightforward condensation reaction, making them accessible for further modifications and functionalizations. Characterization studies have provided valuable insights into the structural and chemical properties of these Schiff bases. Techniques such as FTIR and NMR were used to confirm the formation of the desired compounds and their molecular structures.

In silico studies have complemented the experimental findings by providing theoretical predictions about the properties and drug-like potential applications of Schiff bases derived from 3-aminopropyltrialkoxysilanes. Computational modeling has allowed for the exploration of structure-activity relationships, molecular interactions, and biological activities, guiding further experimental investigations. Overall, the research conducted on these Schiff bases has laid a solid foundation for future studies. The *in silico* antimalarial studies performed on the

compounds showed that the binding energies obtained for all synthesized compounds are lower than those of the reference compounds (clociguanil and cycloguanil), indicating that the synthesized compounds are more stable in the target and may elicit a better therapeutic effect.

REFERENCES

[1] Obasi, N. L., Kaior, G. U., Ibezim, A., Ochonogor, A. E., Rhyman, L., Uahengo, V., Lutter, M., Jurkschat, K., & Ramasami, P. (2017). Synthesis, characterization, antimicrobial screening and in silico studies of Schiff bases derived from trans- para -methoxycinnamaldehyde. *Journal of Molecular Structure*, *1149*, 8–16. https://api.semanticscholar.org/CorpusID:90190990

[2] Schiff, H. (1864). Mittheilungen aus dem Universitätslaboratorium in Pisa: Eine neue Reihe organischer Basen. *Justus Liebigs Annalen Der Chemie*, *131*, 118–119.

[3] Zheng, Y., Ma, K., Li, H., Li, J., He, J., Sun, X., Li, R., & Ma, J. (2009). One Pot Synthesis of Imines from Aromatic Nitro Compounds with a Novel Ni/SiO2 Magnetic Catalyst. *Catalysis Letters*, *128*(3), 465–474. https://doi.org/10.1007/s10562-008-9774-0

[4] Indumathy, B., Gunasekhar, R., Sathiyanathan, P., & Arun, A. P. (2021). Chemistry and Applications of Organosilanes – An Overview. *SGS - Engineering & Sciences*, *1*(01). https://spast.org/techrep/article/view/1451

[5] Anusha, K., Rama, K. & Vineeth, G. (2017). Silane coupling agents – Benevolent binders in composites. *Trends in Biomaterials and Artificial Organs*, *31*(3), 108–113.

[6] Salam, M. A., Al-Amin, M. Y., Salam, M. T., Pawar, J. S., Akhter, N., Rabaan, A. A. & Alqumber, M. A. A. (2023). Antimicrobial Resistance: A Growing Serious Threat for Global Public Health. In *Healthcare,* 11(13). https://doi.org/10.3390/healthcare11131946.

[7] Thakur, S., Jaryal, A. & Bhalla, A. (2024). Recent advances in biological and medicinal profile of schiff bases and their metal complexes: An updated version (2018–2023). *Results in Chemistry*, *7*, 101350. https://doi.org/https://doi.org/10.1016/j.rechem.2024.101350

[8] Ibeji, C., Ukogu, K., Kelani, M., Ebuka, A., Nnamdi, O., Ogundare, S., Maguire, G. & Kruger, G. (2022). Synthesis, Crystal structure, Photoluminescence Properties and Quantum mechanics Studies of Two Schiff Bases of 2-amino-p-cresol. *Journal of Molecular Structure*, *1262*. https://doi.org/10.1016/j.molstruc.2022.13304.

[9] Hadni, H., Mazigh, M. & Hallaoui, M. (2019). QSAR and Molecular docking studies of 4-anilinoquinoline-triazine hybrids as pf-DHFR inhibitors. *Mediterranean Journal of Chemistry*, *8*, 84–93. https://doi.org/10.13171/mjc8219040407hh

[10] Huey, R. & Morris, G. (2008). *Using AutoDock with AutoDockTools: A Tutorial*.

[11] Eberhardt, J., Diogo, S.-M., Andreas, T. & StefanoForli. (2021). *AutoDock Vina 1.2.0: New Docking Methods, Expanded Force Field, and Python Bindings*. https://doi.org/10.26434/chemrxiv.14774223.v1

[12] Singh, G. (2021). *In silico docking analysis of betaine aldehyde dehydrogenase2 with pesticides in scented Basmati Rice*. *Online Journal of Bioinformatics,* 22(2), 111-121.

[13] Bandyopadhyay, S., Abiodun, O., Ogboo, B., Kola-Mustapha, A., Attah, E., Edemhanria, L., Kumari, A., Jaganathan, R., & Adelakun, N. (2022). Polypharmacology of some medicinal plant metabolites against SARS-CoV-2 and host targets: Molecular dynamics evaluation of NSP9 RNA binding protein. *J Biomol Struct Dyn*, 40(22): 11467-11483

[14] Bakchi, B., Krishna, A., Sreecharan, E., Ganesh, V., Niharika, M., Maharshi, S., Babu, P., Sigalapalli , D. K., Bhandare, R. R. B. & Shaik, A. (2022). An Overview on Applications of SwissADME Web Tool in the Design and Development of Anticancer, Antitubercular and Antimicrobial agents: A Medicinal Chemist's Perspective. *Journal of Molecular Structure*, *1259*, 132712. https://doi.org/10.1016/j.molstruc.2022.132712

[15] Zhang, L., Ai, H., Chen, W., Yin, Z., Hu, H., Zhu, J., Zhao, J., Zhao, Q. & Liu, H. (2017). CarcinoPred-EL: Novel models for predicting the carcinogenicity of chemicals using molecular fingerprints and ensemble learning methods. *Scientific Reports*, *7*. https://doi.org/10.1038/s41598-017-02365-0.

[16] Kim, Y., & Chen, J. (2018). Molecular structure of human P-glycoprotein in the ATP-bound, outward-facing conformation. *Science (New York, N.Y.)*, *359*(6378), 915–919. https://doi.org/10.1126/science.aar7389.

[17] Zhang, J.X., Qi, M.J., Shi, M.Z., Chen, J.J., Zhang, X.Q., Yang, J., Zhang, K.Z., Han, Y.L. and Guo, C. (2019). Effects of Danhong injection, a traditional Chinese medicine, on nine cytochrome P450 isoforms in vitro. *Biomedical Chromatography,* (4),44-54 https://doi.org/10.1002/bmc.4250.

Supplementary Materials

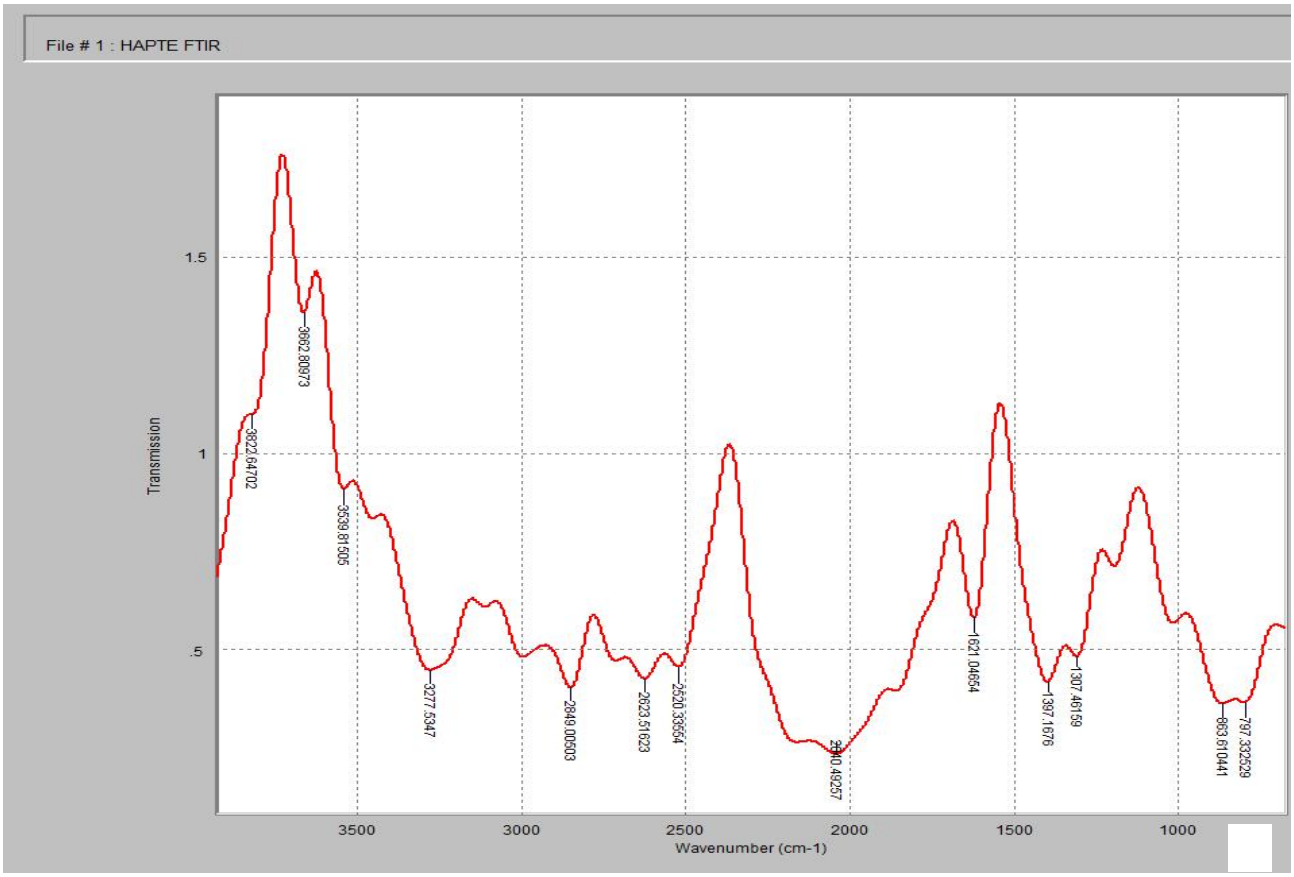

Figure S1: FTIR Spectrum of HAPTE

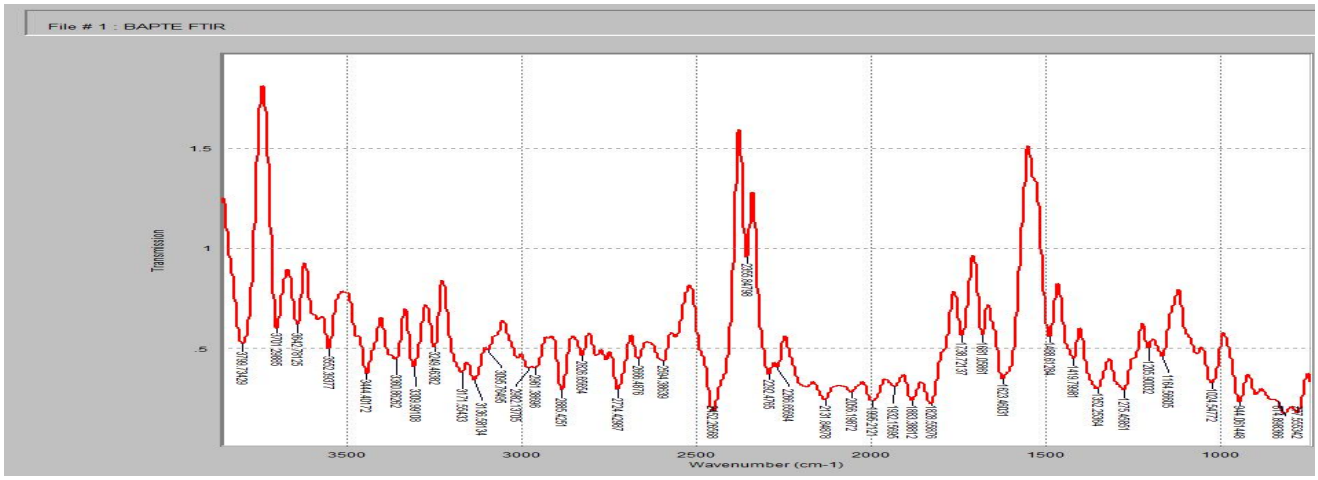

Figure S2: FTIR Spectrum of BAPTE

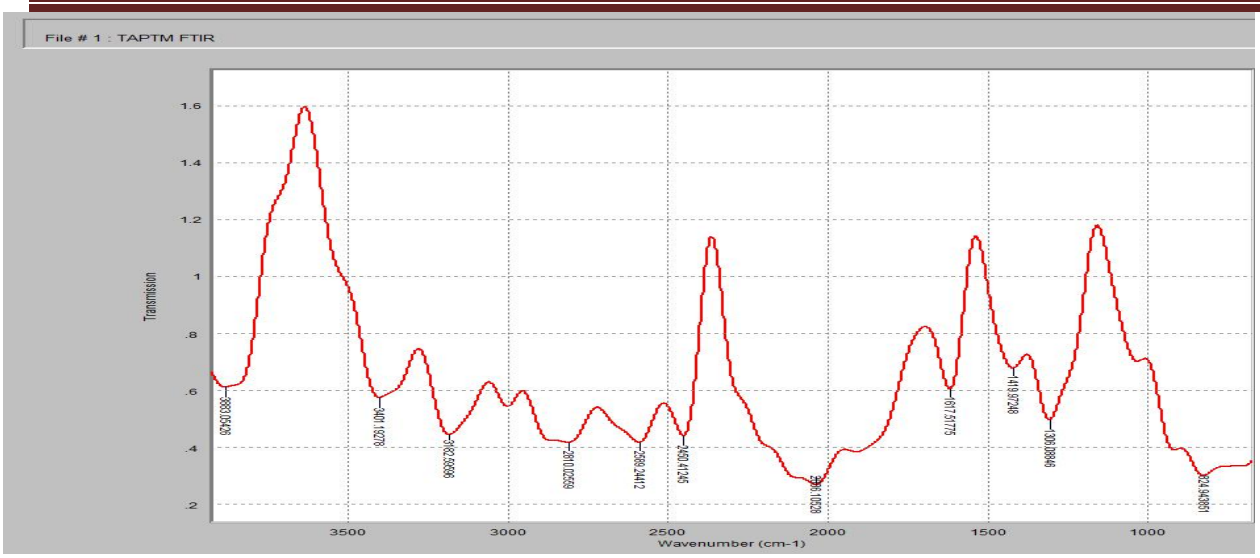

Figure S3: FTIR Spectrum of TAPTM

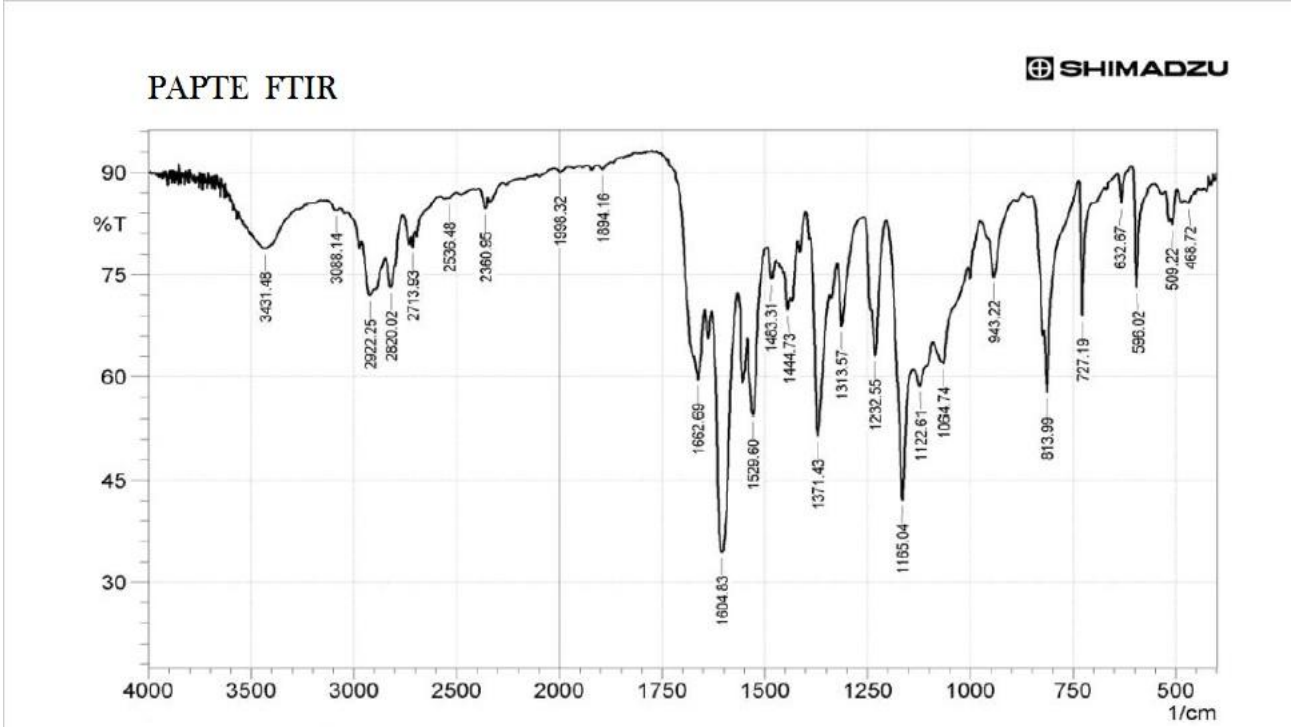

Figure S4: FTIR Spectrum of PAPTE

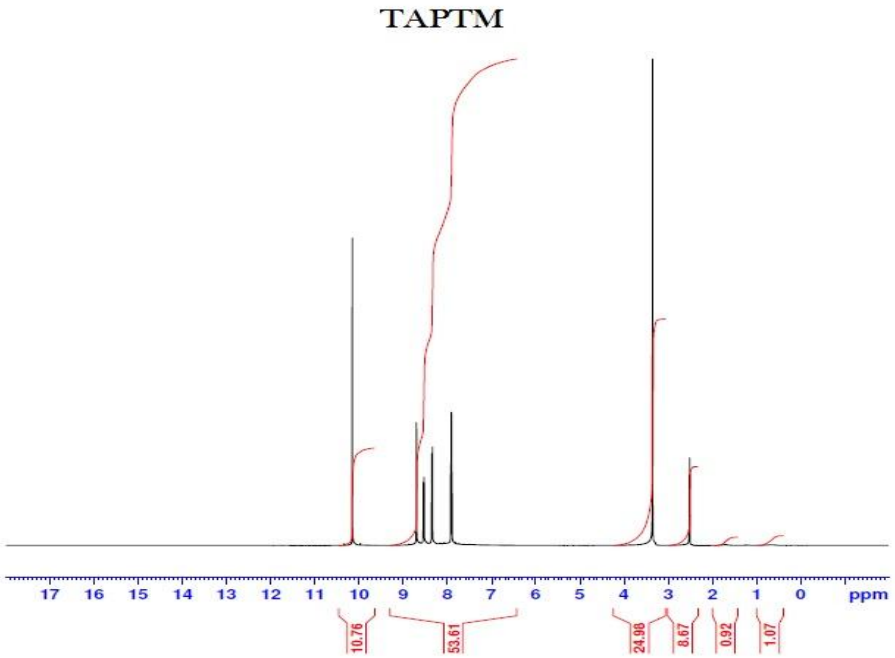

Figure S5: [1]HNMR Spectrum of TAPTM

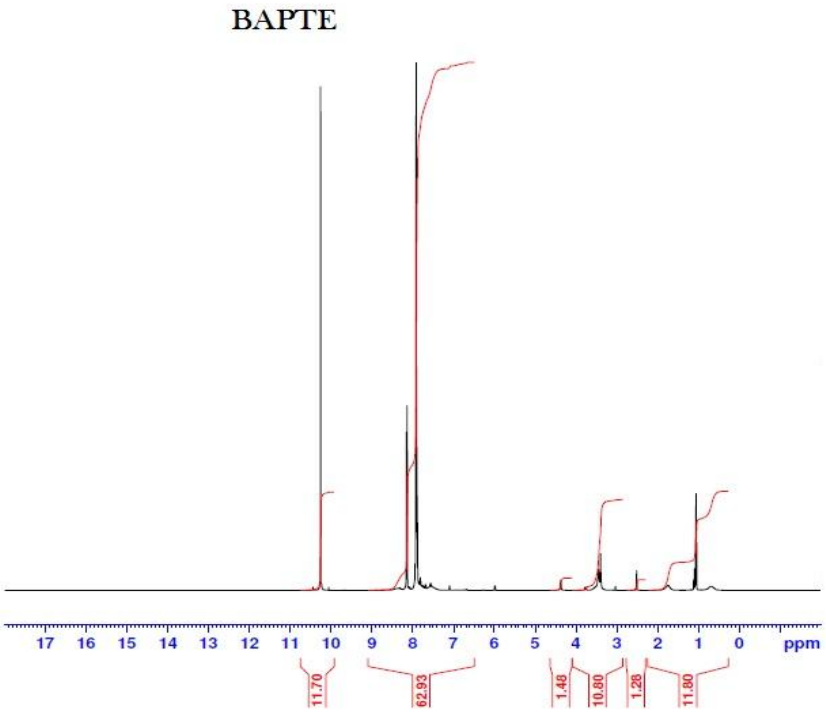

Figure S6: [1]HNMR Spectrumof BAPTE

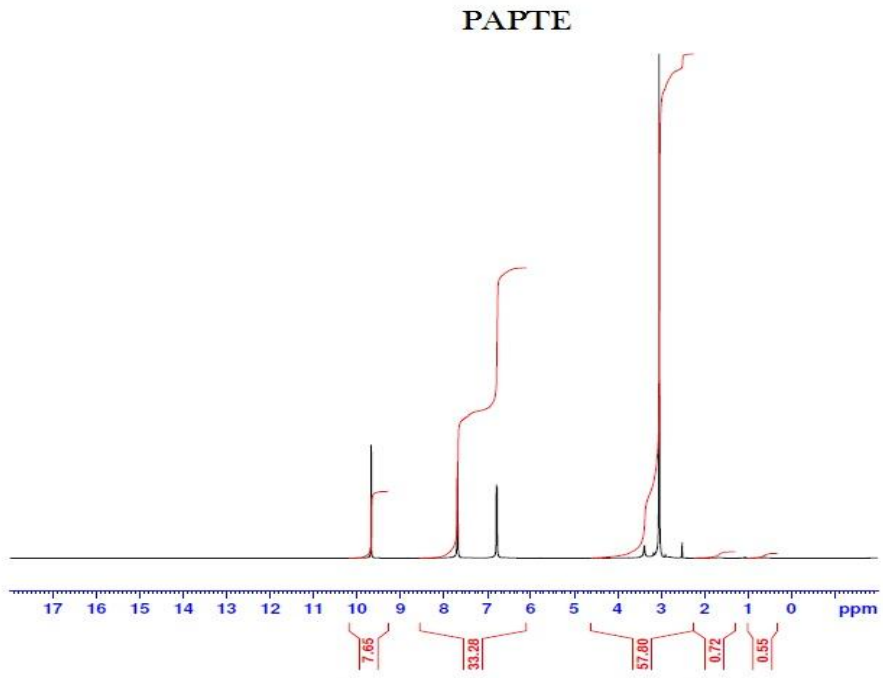

Figure S7: [1]HNMR Spectrum of PAPTE

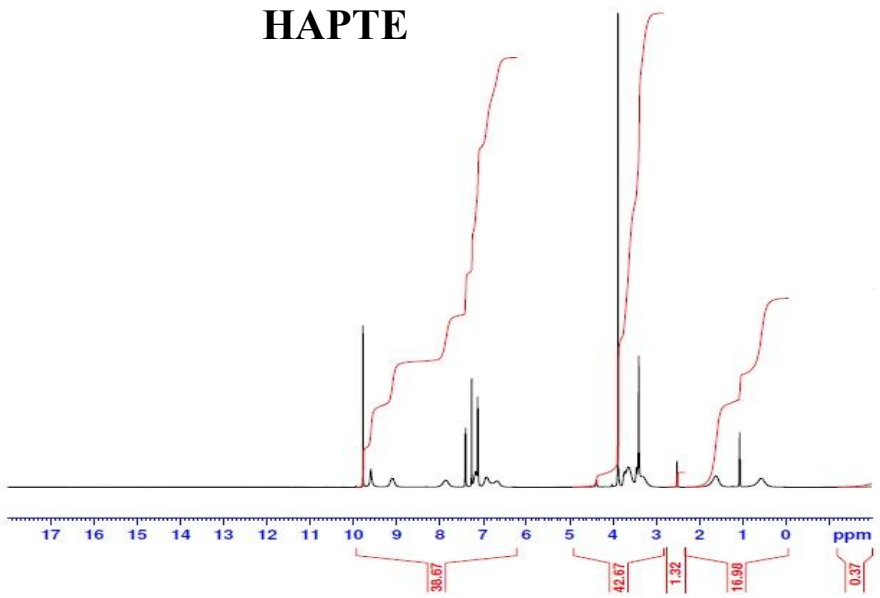

Figure S8: [1]HNMR Spectrum of HAPTE

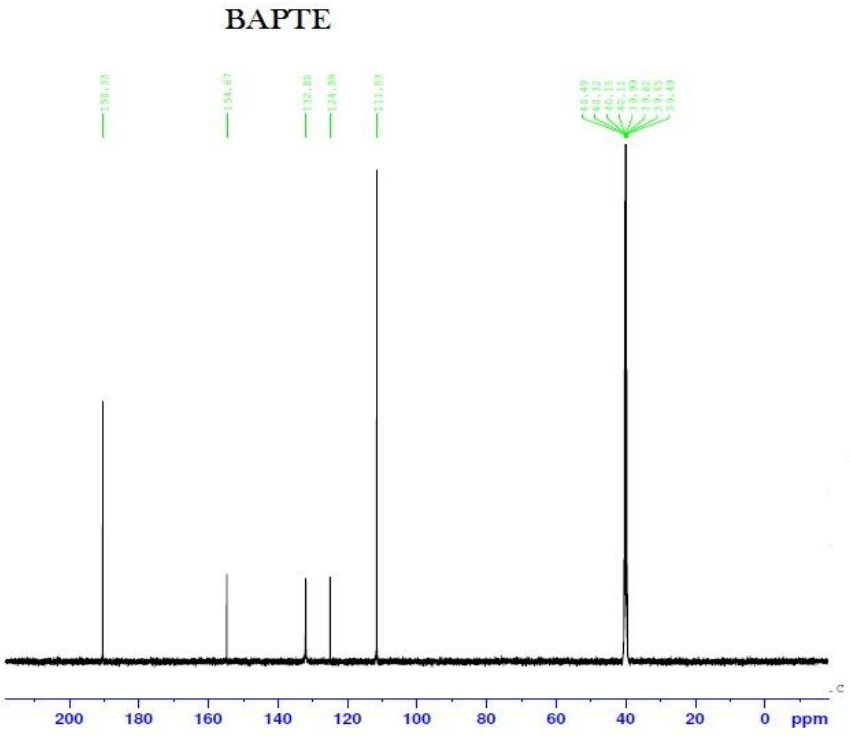

Figure S9: ^{13}C NMR Spectrum of BAPTE

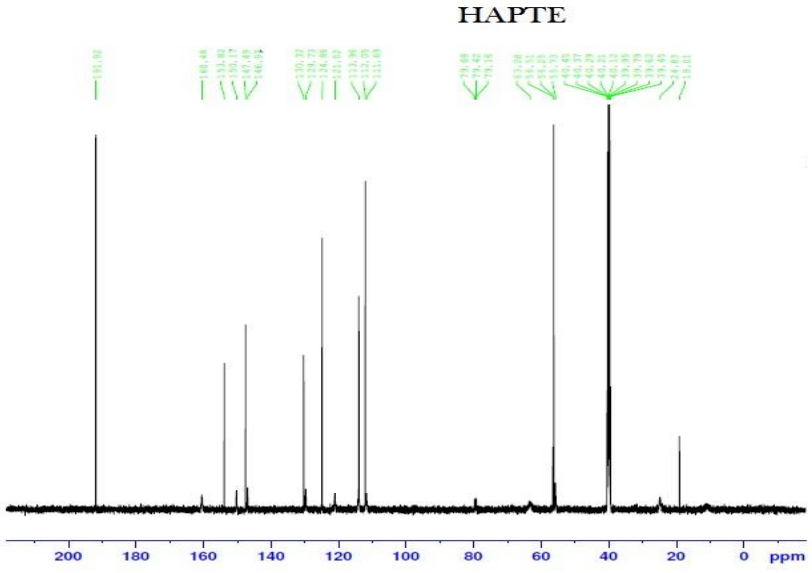

Figure S10: ^{13}C NMR Spectrum of HAPTE

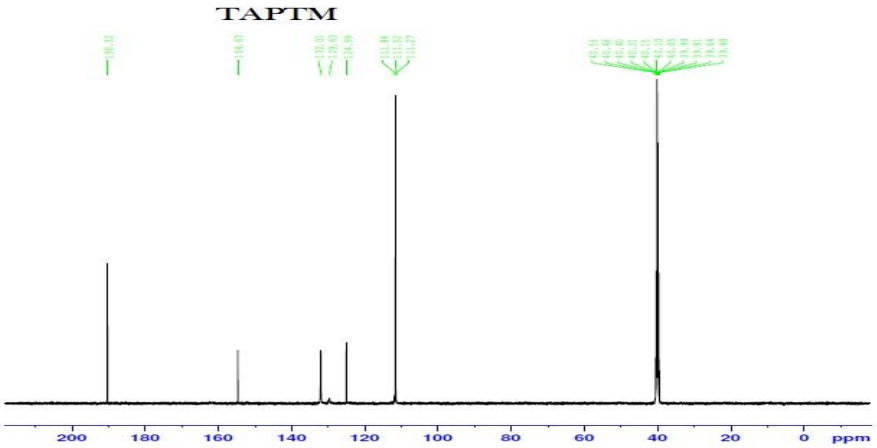

Figure S11: ^{13}C NMR Spectrum of TAPTM

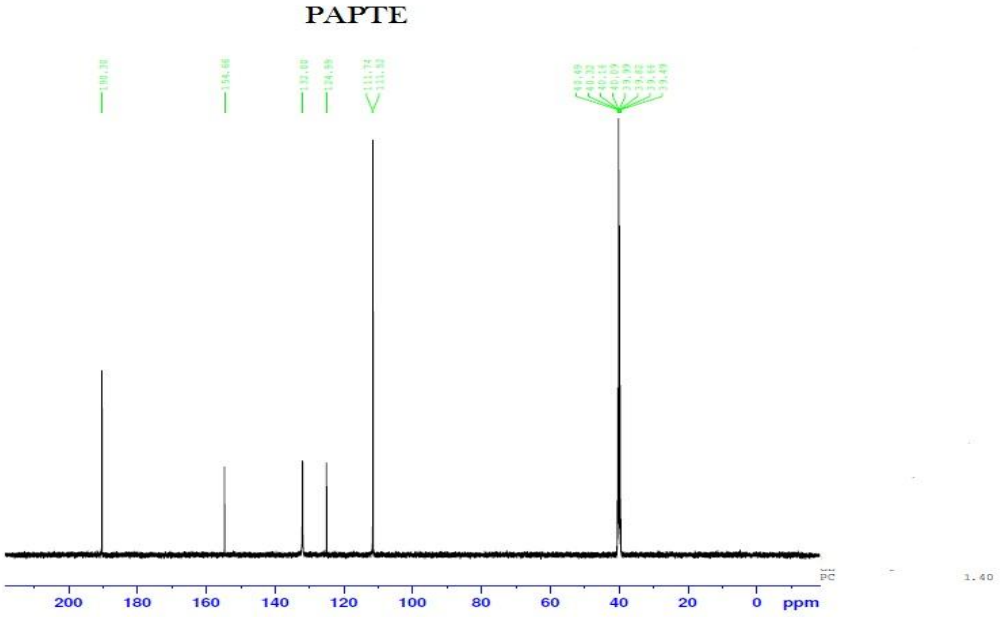

Figure S12: ^{13}C NMR Spectrumof PAPTE